

New Photosensitizers Based upon $[\text{Fe}(\text{L})_2(\text{CN})_2]$ and $[\text{Fe}(\text{L})_3]$ (L = Substituted 2,2'-Bipyridine): Yields for the Photosensitization of TiO_2 and Effects on the Band Selectivity

Suzanne Ferrere

Center for Basic Sciences, National Renewable Energy Laboratory, 1617 Cole Boulevard,
Golden, Colorado 80401

Received November 9, 1999. Revised Manuscript Received February 16, 2000

Our recent report of the sensitization of TiO_2 by $[\text{Fe}(4,4'\text{-dicarboxylic acid-2,2'-bipyridine})_2(\text{CN})_2]$ introduced iron(II) bipyridyl complexes as fundamentally interesting and practical alternatives to their ruthenium analogues in the dye-sensitized solar cell (Ferrere and Gregg, *J. Am. Chem. Soc.* **1998**, *120*, 843). Here we detail how structural changes to the bipyridyl ligand L in $[\text{Fe}(\text{L})_2(\text{CN})_2]$ affect photosensitization yields. We also explore the effect of solvent and solvent additives on the unique absorbance band selectivity of $[\text{Fe}(4,4'\text{-dicarboxylic acid-2,2'-bipyridine})_2(\text{CN})_2]$ on TiO_2 . We demonstrate that solvent conditions can affect the relative photocurrent contributions from the two absorption bands of the complex, and suggest that it is related to changes in driving force for electron injection from the lower energy MLCT band.

Introduction

Sensitization of UV-absorbing semiconductors to the longer wavelengths of the solar spectrum can be achieved by charge injection from visible light absorbing molecules which are associated with the surface of the semiconducting material. The principle has for many years been applied in photographic and xerographic processes. Recently, a solar cell in which titanium dioxide nanoparticles are sensitized by the complex $[\text{Ru}(4,4'\text{-dicarboxylic acid-2,2'-bipyridine})_2(\text{NCS})_2]$, hereafter referred to as "N3", has demonstrated solar conversion efficiencies of 10–12%; its development has advanced the dye-sensitized solar cell from a fundamentally interesting photoelectrochemical system into a viable solar cell technology.¹ Moreover, the sensitization mechanism—a subpicosecond electron-transfer presumed to occur from upper excited states of N3 into the conduction band of the TiO_2 ^{2–4}—compels us to revise previous notions about the excited-state reactivity of metal bipyridyl complexes.

Ruthenium trisbipyridyl complexes have been extensively investigated as photosensitizers because their lowest excited states are long-lived (nanosecond to microsecond) metal-to-ligand charge transfer (MLCT) states that can participate in electron- and energy-transfer reactions.⁵ Ironically, most bisbipyridyl ana-

logues such as N3 were not considered good photosensitizers because their lowest excited states are often ligand field (LF) in nature. Although visible photoexcitation initially populates an MLCT state, the low lying LF states provide deactivation pathways which promote ultrafast (picosecond to nanosecond), nonradiative decay of the MLCT state; this mechanism can compete with possible inter- and intramolecular electron-transfer pathways from the MLCT state.⁶

In the dye-sensitized cell, electron transfer from the excited states of adsorbed sensitizers to the conduction band of TiO_2 occurs within hundreds of femtoseconds.^{2–4} The time scale of electron injection, and its near unity quantum efficiency, imply that this electron transfer occurs from initially populated, nonrelaxed excited states. This finding confutes long-held assumptions about excited state reactivity in metal bipyridyl complexes. Previous notions that electron transfer occurs exclusively from the lowest excited-state directed the choice of sensitizing molecules on the basis of emissive properties—including the emission lifetime, emission quantum yield, and the energetics of the emitting state. However, for electron transfer occurring from initially populated states, as in the dye sensitized cell, it may be the absorptive properties that matter most. This changes the entire perspective of what makes a "good" sensitizer.

These developments are exciting for a number of reasons and open up new possibilities for both fundamental and applied work in molecular photoconversion. First, it justifies reinvestigation of the many classes of

(1) Nazeeruddin, M. K.; Kay, A.; Rodicio, I.; Humphry-Baker, R.; Müller, E.; Liska, P.; Vlachopoulos, N.; Grätzel, M. *J. Am. Chem. Soc.* **1993**, *115*, 6382–6390.

(2) Tachibana, Y.; Moser, J. E.; Grätzel, M.; Klug, D. R.; Durrant, J. R. *J. Phys. Chem.* **1996**, *100*, 20056–20062.

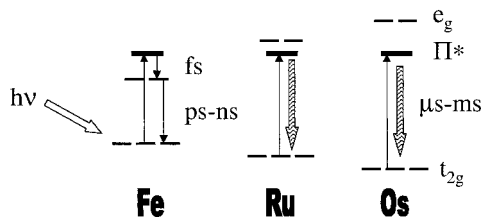
(3) Ellingson, R. J.; Asbury, J. B.; Ferrere, S.; Ghosh, H. N.; Sprague, J. R.; Lian, T.; Nozik, A. J. *J. Phys. Chem. B* **1998**, *102*, 6455–6458.

(4) Hannappel, T.; Burfeindt, B.; Storck, W.; Willig, F. *J. Phys. Chem. B* **1997**, *101*, 6799–6802.

(5) Juris, A.; Balzani, V.; Barigelletti, F.; Campagna, S.; Belser, P.; Von Zelewsky, A. *Coord. Chem. Rev.* **1988**, *84*, 85–277.

(6) Kalyanasundaram, K. *Photochemistry of Polypyridine and Porphyrin Complexes*; Academic Press: New York, 1992.

Scheme 1. Comparative Excited State Orbital Ordering in Octahedral Iron, Ruthenium, and Osmium Bipyridyl Complexes



molecules previously disregarded as photosensitizers because of poor photophysical properties, like short-lived or nonemissive excited states. Second, our fundamental understanding of metal bipyridyl complexes—that photochemical processes are inherently limited to the lowest excited state—have been challenged and demand re-evaluation. Analyses of molecular electron transfer systems usually assume vibrationally relaxed, lowest excited states. From a practical standpoint, this presumption builds in limitations to energy conversion and quantum yields, since relaxation from the Franck–Condon state may involve a decrease in both parameters. Finally, although electron and energy transfer between discrete molecular states is well characterized for numerous molecular donor–acceptor pairs, the parameters which control electron transfer from the discrete state of a dye molecule to a semiconductor’s continuum of states are not well understood.

The aforementioned reasons prompted our investigation of iron(II) bipyridyl complexes as photosensitizers. Iron, ruthenium, and osmium are in the same column of the periodic table but as a first row transition metal, iron has the weakest ligand field (smallest t_{2g} – e_g^* splitting) and osmium, a third row metal, has the strongest ligand field (largest t_{2g} – e_g^* splitting). The resulting orbital ordering for a generic octahedral or pseudooctahedral metal–bipyridyl complex (the bipyridyl π^* level is considered constant) is shown in Scheme 1. For all complexes, visible light excitation prompts an MLCT $t_{2g} \rightarrow \pi^*$ transition. For osmium and ruthenium, the e_g^* orbitals are substantially higher than the π^* orbitals, whereas for iron, the e_g^* orbitals are lower in energy than the π^* orbitals and comprise the lowest excited state orbitals. Not only do iron’s low lying LF states shorten MLCT lifetimes as discussed above, but population of the e_g^* orbital spatially removes the electron from the bipyridyl ligand (which in most cases is proximal to the acceptor). Thus, population of LF states lowers the excited-state energy, uncouples the excited electron from possible quenching pathways, and can render the complex unstable since the e_g^* orbitals are antibonding.

While thorough investigations of the photochemistry and photophysics of iron, ruthenium, and osmium bipyridyl complexes in the 1970s spurred on the widespread application of ruthenium trisbipyridine to photosensitization reactions, they dissuaded similar usage of iron trisbipyridine because of the reasons discussed above.⁷ However, we recently demonstrated that [Fe(4,4′-dicarboxylic acid-2,2′-bipyridine)₂(CN)₂] can sen-

sitize nanocrystalline TiO₂ in a dye-sensitized solar cell device.⁸ Furthermore, the sensitization was shown to be wavelength dependent: although the complex exhibits two MLCT absorption bands, sensitization was much more efficient from the higher energy transition. While the photophysical behavior of the complex in itself implies that sensitization occurs from upper excited states, the wavelength dependence provided even stronger evidence that sensitization was occurring from upper excited states.

We have now prepared a series of complexes [FeL₃] and [FeL₂(CN)₂], where L is a substituted 2,2′-bipyridine. Here we characterize their behavior as adsorbed dyes on nanocrystalline TiO₂. We discuss how their solution solvatochromism translates onto a film, compare solar conversion efficiencies for the whole series, and discuss how solvent conditions affect overall photoconversion efficiencies. Furthermore, solvent effects on the relative conversion efficiencies for the two MLCT absorption transitions in the FeL₂(CN)₂-type complexes are discussed.

Experimental Section

Materials and Methods. All reagents were of commercially available purest grade and, unless otherwise indicated, obtained from Aldrich Chemical Co. Absorbance spectra were measured on a Hewlett-Packard 8453 UV–vis spectrophotometer. Colloidal TiO₂ was prepared by the hydrolysis of titanium isopropoxide in acetic acid as previously described.⁹

Preparation of Complexes. The syntheses and electrochemical and absorption data for the complexes are provided as Supporting Information. The ligand structures and nomenclature can also be found in the Supporting Information.

Film Preparation and Dye Adsorption. Nanocrystalline TiO₂ films were prepared as previously described.¹⁰ In summary, adhesive tape strips were placed on the long edges of a 5 cm × 4 cm piece of F-doped SnO₂ conducting glass (LOF) which had been scored into 1 × 2 cm electrodes. The TiO₂ colloid was spread over the glass with a glass rod; the tape strips help to make a distinct film edge and leave a small area of bare glass where electrical contact can be made. The films were made using one thickness of tape, which results in films that are typically ~5 μm thick. The films were sintered at 450 °C for 1 h. Once cooled, the films were placed into methanolic or acetonitrile solutions (depending on the solubility) containing 0.02 M chenodeoxycholic acid and ~10^{−4} M iron complexes. Typically, the [FeL₂(CN)₂] complexes and their TBA⁺ salts were soluble in methanol, whereas the PF₆[−] salts of [FeL₃] were soluble in acetonitrile. To adsorb [Fe(4,4′-bis-(hydroxymethyl)-2,2′-bipyridine)₂(CN)₂] onto TiO₂, the film was dipped into a ~1:1 acetonitrile/methanol solution of the complex containing no chenodeoxycholic acid. Film absorbance measurements were made by pressing the film to a piece of microscope slide glass, applying solvent between to decrease light scattering, and holding them together with a binder clip.

Incident Photon-to-Current Efficiency (IPCE) Measurements. Incident-photon-to-current efficiency (IPCE) spectra were generated using LabVIEW Version 4.0 programs written for Macintosh. Solar cells were prepared in a sandwich cell configuration, using a counter electrode of deposited platinum as described in Ferrere and co-workers.¹¹ The cells were illuminated through the TiO₂ electrode with monochro-

(8) Ferrere, S.; Gregg, B. A. *J. Am. Chem. Soc.* **1998**, *120*, 843–844.

(9) Zaban, A.; Ferrere, S.; Sprague, J.; Gregg, B. A. *J. Phys. Chem. B* **1997**, *101*, 55–57.

(10) Zaban, A.; Ferrere, S.; Gregg, B. A. *J. Phys. Chem. B* **1998**, *102*, 452–460.

(11) Ferrere, S.; Zaban, A.; Gregg, B. A. *J. Phys. Chem. B* **1997**, *101*, 4490–4493.

(7) Creutz, C.; Chou, M.; Netzel, T. L.; Okumura, M.; Sutin, N. *J. Am. Chem. Soc.* **1980**, *102*, 1309–1319.

matic light (>400 nm) from a xenon arc lamp (PTI, model A 1010) and the current was monitored by a Keithley 236 source measure unit. Absorbed photon-to-current efficiency (APCE) spectra were obtained by dividing the IPCE by the real absorbance ($1-10^{-\text{measured } A}$) of the film. The APCE for bare TiO_2 was subtracted from the complexes' APCE spectra.

Results

Complex Adsorption. The complexes adsorb to the nanocrystalline TiO_2 films via the acid, ester, or alcohol substituents on the bipyridyl ligands. The TiO_2 films do not adsorb dye from solutions of $[Fe(4,4'$ -dimethyl-2,2'-bipyridine) $_2(CN)_2]$, indicating that adsorption of $[FeL_2(CN)_2]$ species occurs exclusively through the linking groups on the bipyridyl ligands and not via the cyano ligand. Except where noted, the $[FeL_2(CN)_2]$ complexes have very similar extinction coefficients, regardless of L.

The extent of adsorption of the complexes was found to be dependent upon the adsorbing group, the protonation state of the adsorbing group, and in some cases, the solvent and/or additives used in the adsorption process. The complex $[Fe(4,4'$ -bis(hydroxymethyl)-2,2'-bipyridine) $_2(CN)_2]$ adsorbed most weakly to the surface ($A_{\text{max}} \sim 0.15$). To get any of the complex adsorbed onto a film, it was necessary to use 1:1 acetonitrile:methanol and to exclude chenodeoxycholic acid from the adsorption solution; presumably, both the additive and methanol can compete with the dye for adsorption sites on the surface. The tris-bipyridyl complex containing the same ligand, $[Fe(4,4'$ -bis(hydroxymethyl)-2,2'-bipyridine) $_3]$ - $[PF_6]_2$, adsorbed strongly to the films (acetonitrile, no chenodeoxycholic acid).

Films of TiO_2 dipped in a methanol solution of $[Fe(4,4'$ -dicarboxylic acid-2,2'-bipyridine) $_2(CN)_2]$ ($A_{\text{max}} \sim 1$) typically had twice the absorbance of films dipped in $[TBA^+]_4[Fe(4,4'$ -dicarboxylate-2,2'-bipyridine) $_2(CN)_2]$, despite the much greater solubility of the TBA^+ form in methanol. In solution there are differences in the absorbance maxima and relative extinction coefficients for the protonated and unprotonated species. However, films prepared from the two solutions have identical spectra, which implies that the complex adsorbs to the films in the same form. Furthermore, when the solution contained chenodeoxycholic acid (0.02 M), the dye adsorbed comparably from either protonation state ($A_{\text{max}} \sim 0.8$). Thus, the observed variance in film absorbance is likely due to differences in dye uptake, which is greater from acidic solutions because of the more positive TiO_2 surface charge.

Typically, solutions of $[TBA^+]_4[Fe(4,4'$ -dicarboxylate-2,2'-bipyridine) $_2(CN)_2]$ produced films that had twice as much absorbance at the lower energy MLCT band than films dipped in $[TBA^+]_4[Fe(5,5'$ -dicarboxylate-2,2'-bipyridine) $_2(CN)_2]$. However, when approximate differences in extinction coefficients are considered,¹² the films had similar dye coverages. The complex $[TBA^+]_8[Fe(4,4'$ -diphosphonate-2,2'-bipyridine) $_2(CN)_2]$ adsorbed comparably with $[TBA^+]_8[Fe(4,4'$ -bis(methylphosphonate)-2,2'-bipyridine) $_2(CN)_2]$ ($A \sim 0.3$), which adsorbed more strongly than its nonhydrolyzed analogue, $[Fe(4,4'$ -bis(diethyl methylphosphonate)-2,2'-bipyridine) $_2(CN)_2]$ ($A \sim 0.2$).

Table 1. Absorbance Maxima for $[TBA^+]_4[Fe(4,4'$ -dicarboxylate-2,2'-bipyridine) $_2(CN)_2]$

| solvent | A, nm | |
|----------------------|-------------|--------------|
| | in solution | on TiO_2^a |
| ethanol | 590 | 610 |
| methoxypropionitrile | 594 | 608 |
| chloroform | 595 | 596 |
| dimethyl sulfoxide | 621 | 638 |

^a The film background has been subtracted.

Solution Absorbance vs Film Absorbance and Solvatochromism. Table 1 indicates the absorbance maxima for $[TBA^+]_4[Fe(4,4'$ -dicarboxylate-2,2'-bipyridine) $_2(CN)_2]$ in solution and adsorbed to a TiO_2 film wetted with solvent. The presence of cyano groups imparts solvatochromic behavior, because solvents can interact with the nonbonding electron pair of the cyano nitrogen. The absorption trends in Table 1 are in accord with the acceptor number of the solvent as previously discussed by a number of authors.^{13,14} Solvents with large acceptor numbers tend to withdraw electron density away from the metal center via their association with the cyano ligand, thereby increasing the energy of the MLCT ($t_{2g} \rightarrow \pi^*$) transition compared to a weakly accepting solvent. In all solvents except chloroform, the complex's MLCT absorbance shifts to lower energy when adsorbed. There is a similar magnitude red shift between solution spectra and action spectra for ruthenium complexes adsorbed through 4,4'-dicarboxylic acid-2,2'-bipyridine onto TiO_2 . The shift has been attributed to delocalization of the bipyridyl π orbitals by electronic overlap with the TiO_2 conduction band.¹ It is also possible that adsorption of $[TBA^+]_4[Fe(4,4'$ -dicarboxylate-2,2'-bipyridine) $_2(CN)_2]$ to TiO_2 changes the electron density of the ligand ($-CO_2Ti^{IV}$ is more electron withdrawing than $-CO_2^-$) and that this more localized effect causes the red shift.¹²

Acid addition to an aprotic solution of $[Fe(4,4'$ -dicarboxylate-2,2'-bipyridine) $_2(CN)_2]$ shifts the MLCT absorbance to higher energy, whereas acid addition to a protic solution shifts the absorbance to lower energy.¹² The contrasting effect is probably due to differences in the solvation of the carboxylate groups on the bipyridyl ligand. When the carboxy groups are "tied up" by adsorption to the TiO_2 surface, the complex behaves more like $[Fe(4,4'$ -dimethyl-2,2'-bipyridine) $_2(CN)_2]$ in solution, that is, the solvatochromism is wholly due to effects at the cyano ligands. In fact, for TiO_2 -adsorbed $[Fe(4,4'$ -dicarboxylate-2,2'-bipyridine) $_2(CN)_2]$, acid addition has very little effect on the absorbance spectra both in protic and aprotic solvents.

Sensitization of TiO_2 by $[Fe(4,4'$ -dicarboxylate-2,2'-bipyridine) $_2(CN)_2]$. Figure 1 shows the APCE spectrum for $[Fe(4,4'$ -dicarboxylate-2,2'-bipyridine) $_2(CN)_2]$ on TiO_2 compared to its absorbance spectrum. Although the complex's two MLCT bands have very similar absorbances, their relative contributions to the action spectra are quite different; that is, the quantum yield for the higher energy (418 nm) transition is nearly 35%, whereas it is only $\sim 12\%$ from the lower energy (~ 612 nm) transition. It should be noted that substan-

(13) Toma, H. E.; Takasugi, M. S. *J. Solution Chem.* **1983**, *12*, 547-561.

(14) Taft, R. W.; Pienta, N. J.; Kamlet, M. J.; Arnett, E. M. *J. Org. Chem.* **1981**, *46*, 661-667.

(12) Ferrere, S. Manuscript in preparation.

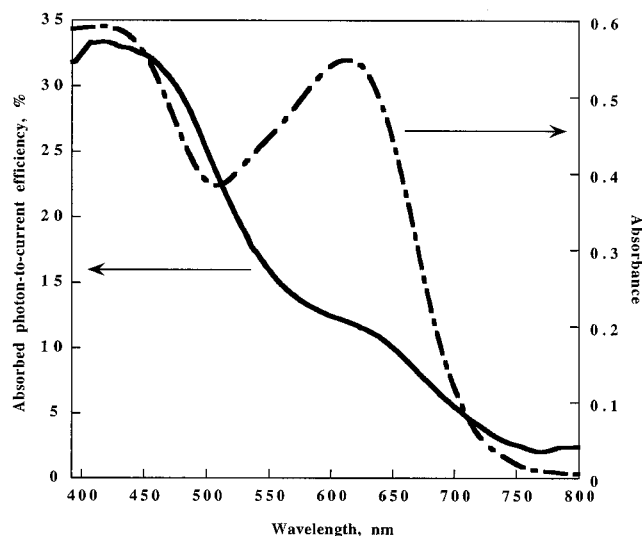


Figure 1. Absorbed photon-to-current efficiency versus wavelength and absorbance spectrum for $[\text{Fe}(4,4'\text{-dicarboxylate-}2,2'\text{-bipyridine})_2(\text{CN})_2]$ on TiO_2 . Solvent is methoxypropionitrile containing 0.5 M LiI and 0.05 M I_2 . The APCE and the absorbance for bare TiO_2 have been subtracted from the respective spectra.

tial gains in quantum efficiency have been made since our initial report of this system.⁸ The primary reason for this is the elimination of 4-*tert*-butylpyridine from the electrolyte solution; the effect of this additive is discussed in detail below.

Comparative Solar Conversion Efficiencies for All Complexes. Here we present how the overall photoconversion efficiencies depend on the linking group and explore the wavelength dependence of the action spectra on adsorbing group. Since the extent of complex adsorption is dependent on numerous factors (*vide supra*), most IPCE data has been converted to APCE spectra to convert the data from a device efficiency to a quantum efficiency for the complex in the device. Where the APCE are very dissimilar, normalized IPCE spectra are presented, to compare relative contributions from the two MLCT absorbance bands to the action spectra.

Dependence on Position of Adsorbing Group: L = 4,4'-Dicarboxylic acid-2,2'-bipyridine vs L = 5,5'-Dicarboxylic acid-2,2'-bipyridine. Figure 2 indicates the APCE spectra for $[\text{Fe}(4,4'\text{-dicarboxylate-}2,2'\text{-bipyridine})_2(\text{CN})_2]$ and $[\text{Fe}(5,5'\text{-dicarboxylate-}2,2'\text{-bipyridine})_2(\text{CN})_2]$ adsorbed onto TiO_2 . Their absorbance spectra are similar, but the 5,5' derivative has a slightly blue shifted spectrum when adsorbed; in addition, the relative extinction of the lower energy transition is smaller for the 5,5' derivative. It can be seen that while the photoconversion efficiency is essentially the same for the two complexes at the higher energy MLCT band, there is virtually no photocurrent contribution from the lower energy MLCT band for $[\text{Fe}(5,5'\text{-dicarboxylate-}2,2'\text{-bipyridine})_2(\text{CN})_2]$.

Dependence on Length of Linker: L = 4,4'-Diphosphonate-2,2'-bipyridine vs L = 4,4'-Bis(methylphosphonate)-2,2'-bipyridine. Figure 3 shows the APCE spectra for $[\text{Fe}(4,4'\text{-diphosphonate-}2,2'\text{-bipyridine})_2(\text{CN})_2]$ and $[\text{Fe}(4,4'\text{-bis(methylphosphonate)-}2,2'\text{-bipyridine})_2(\text{CN})_2]$. Structurally, the complexes differ by the presence or absence of a methylene spacer between the bipyridyl ring and the phosphonate adsorbing group.

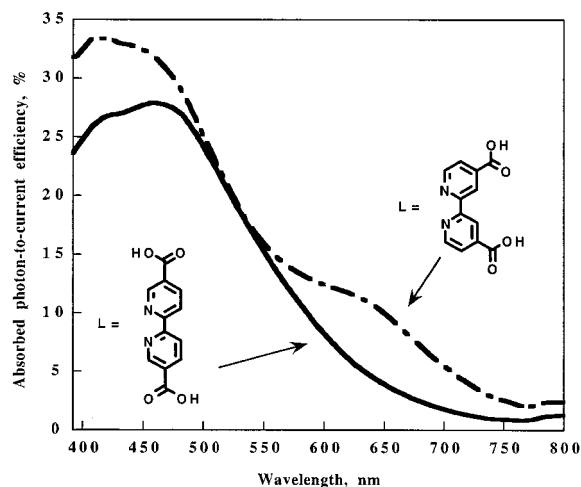


Figure 2. Absorbed photon-to-current efficiency versus wavelength for $[\text{Fe}(4,4'\text{-dicarboxylate-}2,2'\text{-bipyridine})_2(\text{CN})_2]$ and $[\text{Fe}(5,5'\text{-dicarboxylate-}2,2'\text{-bipyridine})_2(\text{CN})_2]$ adsorbed onto TiO_2 . Solvent is methoxypropionitrile containing 0.5 M LiI and 0.05 M I_2 .

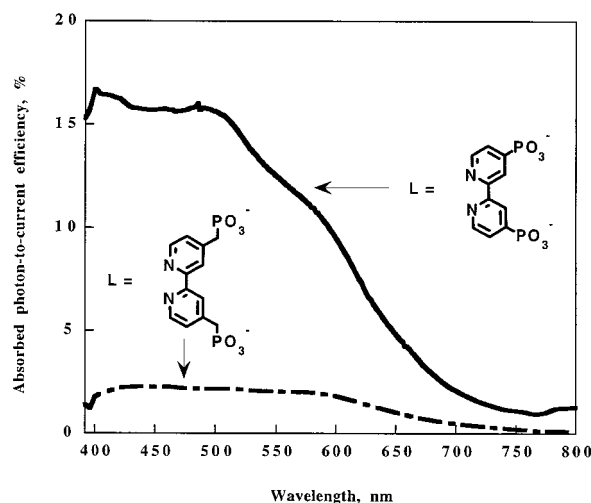


Figure 3. Absorbed photon-to-current efficiency versus wavelength for $[\text{Fe}(4,4'\text{-diphosphonate-}2,2'\text{-bipyridine})_2(\text{CN})_2]$ and $[\text{Fe}(4,4'\text{-bis(methylphosphonate)-}2,2'\text{-bipyridine})_2(\text{CN})_2]$. Solvent is methoxypropionitrile containing 0.5 M LiI and 0.05 M I_2 .

Figure 3 indicates that the overall conversion efficiency is substantially higher when the phosphonate group is linked directly to the bipyridyl ring.

Dependence on Nature of Adsorbing Group: L = 4,4'-Dicarboxy-2,2'-bipyridine vs L = 4,4'-Diphosphonate-2,2'-bipyridine. Figure 4 compares the APCE spectra for $[\text{Fe}(4,4'\text{-diphosphonate-}2,2'\text{-bipyridine})_2(\text{CN})_2]$ and $[\text{Fe}(4,4'\text{-dicarboxylate-}2,2'\text{-bipyridine})_2(\text{CN})_2]$. It can be seen that the overall efficiency is greater for the carboxylated dye. However, it appears as if the phosphonated derivative shows a higher efficiency at lower wavelengths, that is, the action spectrum more closely resembles the absorbance spectrum.

L = 4,4'-Bis(methylphosphonate)-2,2'-bipyridine vs L = 4,4'-Bis(diethyl methylphosphonate)-2,2'-bipyridine vs L = 4,4'-Bis(hydroxymethyl)-2,2'-bipyridine. Figure 5 contains the APCE spectra for the three $[\text{Fe}(\text{L})_2(\text{CN})_2]$ complexes that have a methylene spacer between the bipyridyl ring and the adsorbing group. The absorbance spectrum of adsorbed $[\text{Fe}(4,4'$

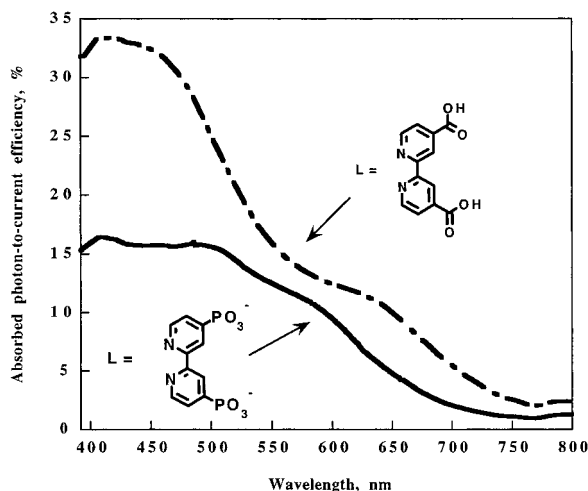


Figure 4. Absorbed photon-to-current efficiency versus wavelength for $[\text{Fe}(4,4'\text{-diphosphonate-2,2'-bipyridine})_2(\text{CN})_2]$ and $[\text{Fe}(4,4'\text{-dicarboxylate-2,2'-bipyridine})_2(\text{CN})_2]$. Solvent is methoxypropionitrile containing 0.5 M LiI and 0.05 M I_2 .

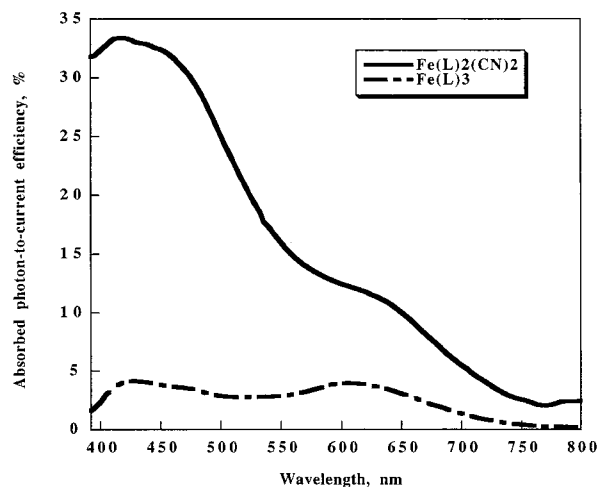


Figure 6. Absorbed photon-to-current efficiency versus wavelength for $[\text{Fe}(4,4'\text{-dicarboxy-2,2'-bipyridine})_3]$ and $[\text{Fe}(4,4'\text{-dicarboxy-2,2'-bipyridine})_2(\text{CN})_2]$. Solvent is methoxypropionitrile containing 0.5 M LiI and 0.05 M I_2 .

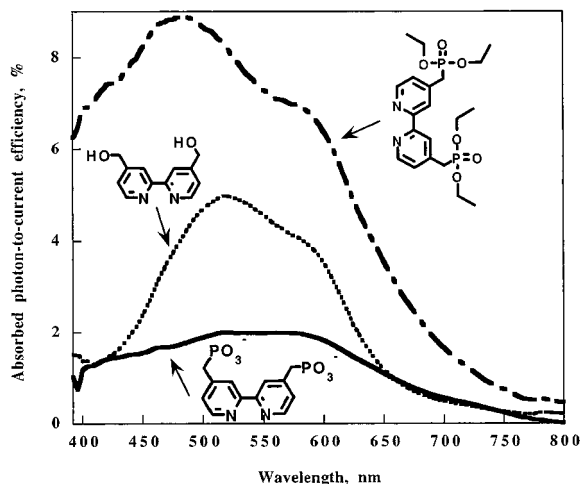


Figure 5. Absorbed photon-to-current efficiency versus wavelength for $[\text{Fe}(\text{L})_2(\text{CN})_2]$ where L = (4,4'-bis(methylphosphonate)-2,2'-bipyridine); 4,4'-bis(diethyl methylphosphonate)-2,2'-bipyridine; and 4,4'-bis(hydroxymethyl)-2,2'-bipyridine. Solvent is methoxypropionitrile containing 0.5 M LiI and 0.05 M I_2 .

bis(diethyl methylphosphonate)-2,2'-bipyridine) $_2(\text{CN})_2]$ is broad with an absorbance maximum ~ 525 nm that is identical to that for adsorbed $[\text{Fe}(4,4'\text{-bis(methylphosphonate)-2,2'-bipyridine})_2(\text{CN})_2]$, and a long wavelength absorption shoulder (~ 600 nm). It is likely that the broader spectrum is due to various states of hydrolysis, as the complex can adsorb either directly as the ester or as the hydrolyzed product, in which case it would be spectrally identical to adsorbed $[\text{Fe}(4,4'\text{-bis(methylphosphonate)-2,2'-bipyridine})_2(\text{CN})_2]$. The APCE shapes for both complexes are similar, although for the hydrolyzed complex it is red shifted from that of the ester. The lowest overall conversion efficiency is for $[\text{Fe}(4,4'\text{-bis(methylphosphonate)-2,2'-bipyridine})_2(\text{CN})_2]$. Although $[\text{Fe}(4,4'\text{-bis(hydroxymethyl)-2,2'-bipyridine})_2(\text{CN})_2]$ is the complex that adsorbs most weakly to the TiO_2 films, it exhibits a higher conversion efficiency than $[\text{Fe}(4,4'\text{-bis(methylphosphonate)-2,2'-bipyridine})_2(\text{CN})_2]$.

Tris vs Bis Complexes: $[\text{Fe}(4,4'\text{-dicarboxy-2,2'-bipyridine})_3]$ vs $[\text{Fe}(4,4'\text{-dicarboxy-2,2'-bipyridine})_2(\text{CN})_2]$. The APCE spectra for these two complexes are

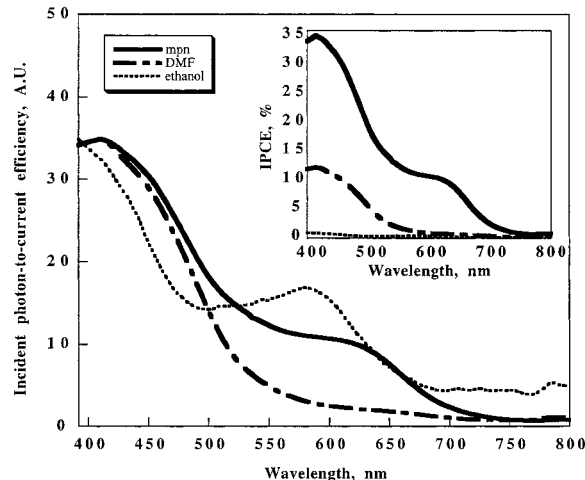


Figure 7. Normalized IPCE spectra for $[\text{Fe}(4,4'\text{-dicarboxylate-2,2'-bipyridine})_2(\text{CN})_2]$ on TiO_2 obtained in three different solvents: methoxypropionitrile (mpn), dimethylformamide (DMF), and ethanol. Electrolyte was 0.5 M LiI and 0.05 M I_2 . The inset shows the uncorrected IPCE spectra.

shown in Figure 6. The bis complex clearly is a much better sensitizer than the tris complex.

Dependence of Action Spectrum Shape: Solvent. The inset of Figure 7 shows the IPCE for $[\text{Fe}(4,4'\text{-dicarboxylate-2,2'-bipyridine})_2(\text{CN})_2]$ on TiO_2 obtained in three different solvents: 3-methoxypropionitrile (mpn), dimethylformamide (DMF), and ethanol. It can be seen that the overall conversion yield is highest in mpn; this solvent also gives the best performance for N3 on TiO_2 . However, a more significant difference among the solvents can be seen upon normalization of the spectra (Figure 7). In DMF, there is virtually no photocurrent contribution from the lower energy MLCT transition. In ethanol, the action spectrum resembles most closely the absorption spectrum, that is, the photocurrent contribution from the two MLCT bands are equally proportional to their absorbances.

Acid/Base Additions. Figure 8 shows the normalized action spectra for $[\text{Fe}(4,4'\text{-dicarboxylate-2,2'-bipyridine})_2(\text{CN})_2]$ on TiO_2 with mpn solvent and when acid or base is added. In the inset of Figure 8 it can be seen

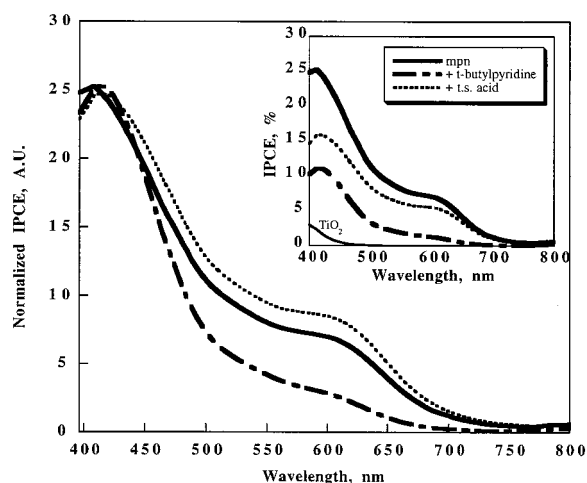


Figure 8. Normalized IPCE spectra for $[\text{Fe}(4,4'\text{-dicarboxylate-}2,2'\text{-bipyridine})_2(\text{CN})_2]$ on TiO_2 obtained in methoxypropionitrile (mpn), in mpn containing 0.2 M 4-*tert*-butylpyridine, and in mpn containing 0.05 M paratoluenesulfonic acid. Electrolyte was 0.5 M LiI and 0.05 M I_2 . The inset shows the uncorrected IPCE spectra and also the IPCE for bare TiO_2 .

that the overall conversion efficiency is diminished by either additive. However, the relative contribution from the lower energy MLCT transition is made greater by the addition of acid. When 4-*tert*-butylpyridine is added, the relative contribution from the lower energy MLCT transition is virtually eliminated.

Discussion and Summary. The spectral dependence of the photocurrent can provide useful information about the injection efficiency of the dye. However, in addition to the injection efficiency (ϕ_{inj}), the IPCE also contains the electron collection efficiency of the device (η_{el}) and the light harvesting efficiency (LHE) of the adsorbed complex:

$$\text{IPCE} = \phi_{\text{inj}} \times \eta_{\text{el}} \times \text{LHE}$$

By dividing out the absorbance spectrum, the LHE is easily factored out to give an APCE. The APCE can be a good relative approximation of injection yields for similar dyes if the TiO_2 films and electrolyte conditions are identical. We have determined the APCE spectra for a series of dyes $[\text{Fe}(\text{L})_2(\text{CN})_2]$ to characterize how structural differences in L affect the injection yield. Unfortunately, structural changes in L cannot be isolated from other complex properties that affect sensitization yields, like electrochemical and spectral properties; the solvatochromism of the dicyano complex only exacerbates this difficulty.¹² However, we offer some reasonable explanations for the trends within the series.

For the series $[\text{Fe}(\text{L})_2(\text{CN})_2]$, the best sensitizer has $\text{L} = 4,4'\text{-dicarboxy-}2,2'\text{-bipyridine}$. It shows higher photoconversion efficiency than the analogous phosphonate complex, and much higher efficiency than all of the complexes in which L has a methylene group between the bipyridyl ring and the adsorbing group. The complex where $\text{L} = 4,4'\text{-diphosphonate-}2,2'\text{-bipyridine}$ exhibits a higher efficiency than the complex with $\text{L} = 4,4'\text{-bis(methylphosphonate)-}2,2'\text{-bipyridine}$. Neither of these results can be explained by simple driving force effects on the injection process; that is, in each comparison, the less efficient complex has a more negative excited-state energy.¹² While we have not done a photophysical study

of the series, it is also unlikely that differences in excited-state lifetimes can account for the observed trends. In fact, $[\text{Fe}(4,4'\text{-dicarboxylate-}2,2'\text{-bipyridine})_2(\text{CN})_2]$ would be predicted to have the shortest lifetime in the series. Instead, it seems more likely that the trends are due to differences in the electronic coupling between the complexes and the semiconductor. The coupling of the complexes to the TiO_2 is mediated by the linkages. Thus, the dye–semiconductor linkage is a crucial parameter for efficient excited-state electron injection from $[\text{Fe}(\text{L})_2(\text{CN})_2]$ complexes. A recent report by Hou and co-workers also found that the photocurrent in devices made from $[\text{Ru}(\text{L})_2(\text{NCS})_2]$ species was dependent upon the type of adsorbing group; however, the absorbance and action spectra of the dyed films were not indicated.¹⁵ Meyer and co-workers examined a series of $[\text{Ru}(\text{dmb})_2(\text{L})]$ complexes on nanocrystalline TiO_2 and found that the complex where $\text{L} = 4\text{-(CH}_2)_3\text{COOH-}4'\text{-(CH}_3\text{)-}2,2'\text{-bipyridine}$ had an IPCE of 26%, whereas the complex in which $\text{L} = 4\text{-(COOH)-}4'\text{-(CH}_3\text{)-}2,2'\text{-bipyridine}$ had an IPCE of 50%.¹⁶ The trisbipyridyl ruthenium complexes are also capable of electron injection from their long-lived lowest excited states, which may explain why the addition of three methylenes between the sensitizer and the adsorbing group only decreased the conversion yield by $\sim 50\%$ in Meyer's study. For the $[\text{Fe}(\text{L})_2(\text{CN})_2]$ species presented here, introduction of a single methylene unit decreases the overall conversion efficiency by more than 80% (Figure 3). It is interesting to note that there may be inherent differences in the linkage dependence of upper versus lower excited state electron injection.

In addition to variance in overall conversion yields of the complexes, we also see some variance in the band selectivity of the injection process. Again, the observation that injection appears to be more efficient from the higher energy MLCT transition than from the lower energy MLCT transition has a number of possible explanations. Here we present evidence that the band selectivity can be affected by both coupling and driving force effects. A unique effect is seen in the comparison between $[\text{Fe}(4,4'\text{-dicarboxylate-}2,2'\text{-bipyridine})_2(\text{CN})_2]$ and $[\text{Fe}(5,5'\text{-dicarboxylate-}2,2'\text{-bipyridine})_2(\text{CN})_2]$. Although they sensitize TiO_2 comparably from the higher energy MLCT band, the 5,5'-derivatized complex shows virtually no photocurrent contribution from the lower energy MLCT band. The two complexes have identical excited-state energies for this transition, so there should be no additional driving force limitation for the 5,5' compared to the 4,4' derivative. Meyer and Bignozzi concluded that $[\text{Ru}(5,5'\text{-dicarboxy-}2,2'\text{-bipyridine})_2(\text{X})_2]$ complexes exhibited lower photosensitization yields than $[\text{Ru}(4,4'\text{-dicarboxy-}2,2'\text{-bipyridine})_2(\text{X})_2]$ complexes because the 5,5' complexes are predicted to undergo faster nonradiative decay, based upon an energy gap argument.¹⁷ However, it is now well-established that injection can compete kinetically with intramolecular relaxation processes.^{2–4} The difference between the two complexes may be related to differences in the electronic

(15) Hou, Y.; Xie, P.; Zhang, B.; Cao, Y.; Xiao, X.; Wang, W. *Inorg. Chem.* **1999**, *38*, 6320–6322.

(16) Heimer, T. A.; D'Arcangelis, S. T.; Farzad, F.; Stipkala, J. M.; Meyer, G. J. *Inorg. Chem.* **1996**, *35*, 5319–5324.

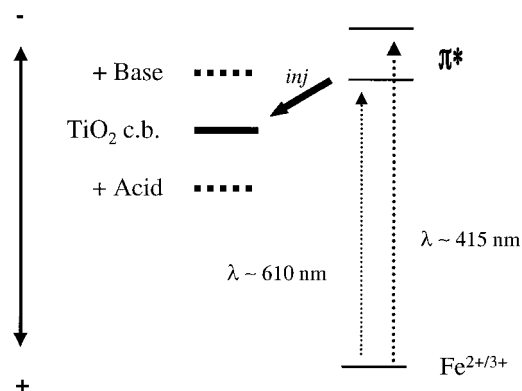
(17) Argazzi, R.; Bignozzi, C. A.; Heimer, T. A.; Castellano, F. N.; Meyer, G. J. *Inorg. Chem.* **1994**, *33*, 5741–5749.

coupling to the surface for the 4,4' and the 5,5' linkage. The transition dipole of the absorbance is directed along the iron–nitrogen bond, and it is a weaker transition in the 5,5' complex.¹² Furthermore, electrochemistry suggests that the 4,4' position is more electron withdrawing and thus may be more effective at directing the excited-state electron density into the semiconductor at this attachment point.

A comparison of $[Fe(4,4'\text{-dicarboxylate-2,2'\text{-bipyridine)}_2(CN)_2]$ and $[Fe(4,4'\text{-dicarboxylate-2,2'\text{-bipyridine)}_3]$ indicates that the dicyano complex is the more effective sensitizer. There are a number of differences between the two complexes, and we reserve explanation until we understand these systems more fully. However, we find the substantially different behavior interesting and note that the differences between tris- and bisruthenium complexes are much smaller.

We also observe that the overall conversion efficiency is affected by solvent and by acid and base additions to the solvent. The overall efficiency differences are likely due to the complex (and still not completely understood) ways in which solvent affects the device. More significant, however, is that the relative photocurrent contribution from the two MLCT bands can be affected by the solvent or by acid/base additions to the solvent. The addition of 4-*tert*-butylpyridine to the methoxypropionitrile solvent has the same qualitative effect as going from methoxypropionitrile to dimethylformamide, a basic solvent; the addition of toluenesulfonic acid to methoxypropionitrile has the same qualitative effect as going from methoxypropionitrile to ethanol, a protic solvent. Basic conditions diminish, whereas acidic conditions increase, the relative contribution from the lower energy MLCT. Although the complex is solvatochromic, the absorption spectrum of the dyed film does not change between the solvents used in this comparison (Table 1). Instead, these effects seem most likely due to changes in driving force for injection which originate in the TiO_2 surface charge; basic conditions move the conduction band negatively, whereas acidic conditions move the conduction band positively (Scheme 2). In this way, the overall driving force for injection is either decreased or increased, respectively. Whereas the higher energy MLCT transition may have substantial overpotential for injection and is unaffected, the lower energy

Scheme 2. Effect of Basic and Acidic Conditions on the Relative Energetics at the $[Fe(4,4'\text{-dicarboxylate-2,2'\text{-bipyridine)}_2(CN)_2]-TiO_2$ Interface



MLCT is sensitive to these slight changes in the conduction band potential.

Finally, we suggest that the development of iron(II) bipyridyl sensitizers should be pursued for both fundamental and practical objectives. It was only recently that this system was recognized for its sensitizing potential, and here we have shown that $[Fe(4,4'\text{-dicarboxylate-2,2'\text{-bipyridine)}_2(CN)_2]$ exhibits relatively high quantum yields for the sensitization of nanocrystalline TiO_2 . Our fundamental understanding of the photophysical behavior of iron(II) bipyridyl systems needs updating, and the unique nature of dye–semiconductor communication demands further investigation. In addition, iron is the most common and cheapest of all metals and thus provides a very practical alternative to ruthenium in sensitizing complexes.

Acknowledgment. I would like to acknowledge the Director's Discretionary Research and Development Program (National Renewable Energy Laboratory) for support of this work and Dr. Brian A. Gregg for helpful discussions.

Supporting Information Available: Structures and syntheses of ligands and complexes, NMR data, electrochemical data, and spectral data. This material is available free of charge via the Internet at <http://pubs.acs.org>.

CM990713K